*Fracture Mechanics of Concrete and Concrete Structures -*
*Recent Advances in Fracture Mechanics of Concrete - B. H. Oh, et al.(eds)*
*ⓒ 2010 Korea Concrete Institute, Seoul, ISBN 978-89-5708-180-8*

# Impact response of post-tensioned and reinforced concrete members with an UHPFRC overlay

K. Habel
*AECOM, 17007 107 Ave, Edmonton, Alberta, Canada*

ABSTRACT: This paper presents analytical analysis of the dynamic behavior of reinforced and post-tensioned concrete slab strips with an ultra high performance fiber-reinforced concrete (UHPFRC) overlay in flexural compression. First, the dynamic equilibrium of 5 large-scale drop weight tests was established to quantify inertia effects in the slab strips. The dynamic equilibrium demonstrated the significant influence of inertia effects during the first 20ms after the impact and allowed verification of consistency of several measurement systems. Then, a mass-spring model was used to determine equivalent static force-deflection curves for each test, which were compared to static test results on comparable slab strips. The slab strips with the UHPFRC overlay in flexural compression showed an increase in apparent strength of up to 18 % due to the dynamic effects. The study demonstrated that the advantageous material behavior of UHPFRC can be well exploited in structural members subject to impact-type loading.

## 1 INTRODUCTION

UHPFRC is a promising material for strengthening and improvement of existing structures. This has been demonstrated for static and long-term behavior (Alaee & Karihaloo 2003, Kunieda et al. 2004, Habel et al. 2006, Habel et al. 2007, Lim & Li 1997). Some studies also show the potential for UHPFRC to withstand impact type loading (Parant & Rossi 2004, Maalej et al. 2005).

In this study, the structural response of reinforced and post-tensioned concrete members with UHPFRC overlay subjected to impact-type loading was investigated. The aim was to evaluate the behavior of those elements under low velocity impact representing cases such as vehicle impact, rock fall or avalanches.

Results of an experimental campaign of drop weight tests on reinforced and post-tensioned slab strips with UHPFRC overlay were previously published in Habel & Gauvreau (2009). The results showed the positive influence of UHPFRC with regard to cracking behavior and resistance. Since important inertia effects occur in dynamic tests, it was necessary to further analyze the tests. The objectives of this paper were to quantify the inertia effects and to analytically determine the equivalent static force-deflection curves of the drop weight tests with the UHPFRC layer in flexural compression presented in Habel & Gauvreau (2009).

The magnitude of the inertia effects was obtained by evaluating the dynamic equilibrium during the tests. The equilibrium also allowed verification of the redundancy between the different measurements during the tests and to examine the validity of the test results. Equivalent static force-deflection curves were determined for the reinforced concrete slab strips with a mass-spring model and then compared to static reference tests.

Previous studies have shown that impact-type loading can be well simulated with analytical mass-spring models, when nonlinear springs are incorporated into the models (Biggs 1964, Bischoff et al. 1990, CEB-FIP 1988, Schlüter 1987). Although these simple tools can only be used to predict overall structural response, they often give sufficient information for use in design.

## 2 TESTS AND TEST RESULTS

Test results were previously published in Habel & Gauvreau (2009). Summarized information is given in the following section.

### 2.1 *Test specimens*

The 3600 mm long reinforced or post-tensioned concrete slab strips had cross-sections according to Figure 1. The names of the slab strips were composed of the cross-section description and a 'D' for drop weight or a 'S' for static tests. Table 1 gives an overview of the tested specimens. All specimens had UHPFRC in flexural compression and no reinforcement in the UHPFRC layer.

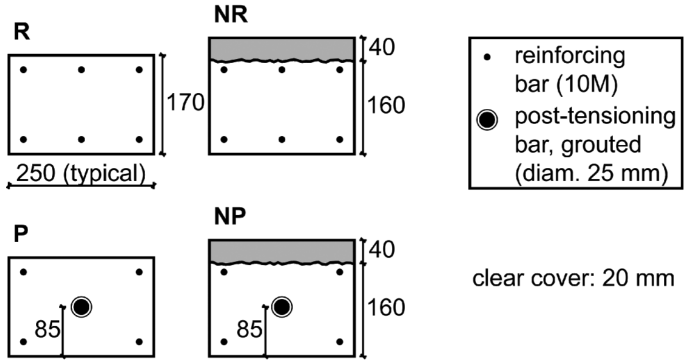


Figure 1. Cross-sections of the specimens.

Table 1. Specimen Overview.

| Name | Concrete substrate reinforcement | UHPFRC layer ($h_U$) |
|---|---|---|
| Drop weight tests | | |
| R+D | reinforced | none |
| NR+D1 | reinforced | 40 mm |
| NR+D2 | reinforced | 40 mm |
| P+D | post-tensioned | none |
| NP+D | post-tensioned | 40 mm |
| Static reference tests | | |
| R+S | reinforced | none |
| NR+S | reinforced | 40 mm |
| NP+S | post-tensioned | 40 mm |

## 2.2 *Materials*

The UHPFRC used is described in Habel et al. (2008). The water/binder-ratio was 0.20 and the steel fiber content was 5.5 Vol-%. The compressive strength, tested on three cylinders (100 mm diameter), was 128 MPa at 28 days and 131 MPa at the age of testing of the composite slab strips (100 days). The uniaxial tensile strength was 11 MPa at a deformation of 0.15%, exhibiting strain-hardening material behavior (Habel & Gauvreau 2006).

The concrete used for the substrate was a conventional concrete provided by a local ready-mix supplier. It had a compressive strength of 33 MPa after 28 days and 37 MPa at the time of testing of the composite slab strips (250 days).

The reinforcing bars in the specimen were 10M bars with a cross section of 100 mm$^2$. Coupon tests indicated a yield strength of 470 MPa with a well-defined yield-plateau and an ultimate strength of 750 MPa. The post-tensioning bars had a cross section of 548 mm$^2$ and a nominal ultimate strength of 1030 MPa. The experimentally determined ultimate strength was 1130 MPa. The post-tensioning force in the post-tensioned slap strips NP and P was approximately 250 kN at the time of testing and was applied on the concrete substrates only (before casting the UHPFRC layer of NP).

The specimens were tested at an average age of the UHPFRC layer of 100 days for the drop weight tests.

## 2.3 *Drop weight tests*

The behavior of the composite slab strips under impact type loading was determined by drop weight tests. The test setup was a three-point bending setup as shown in Figure 2a.

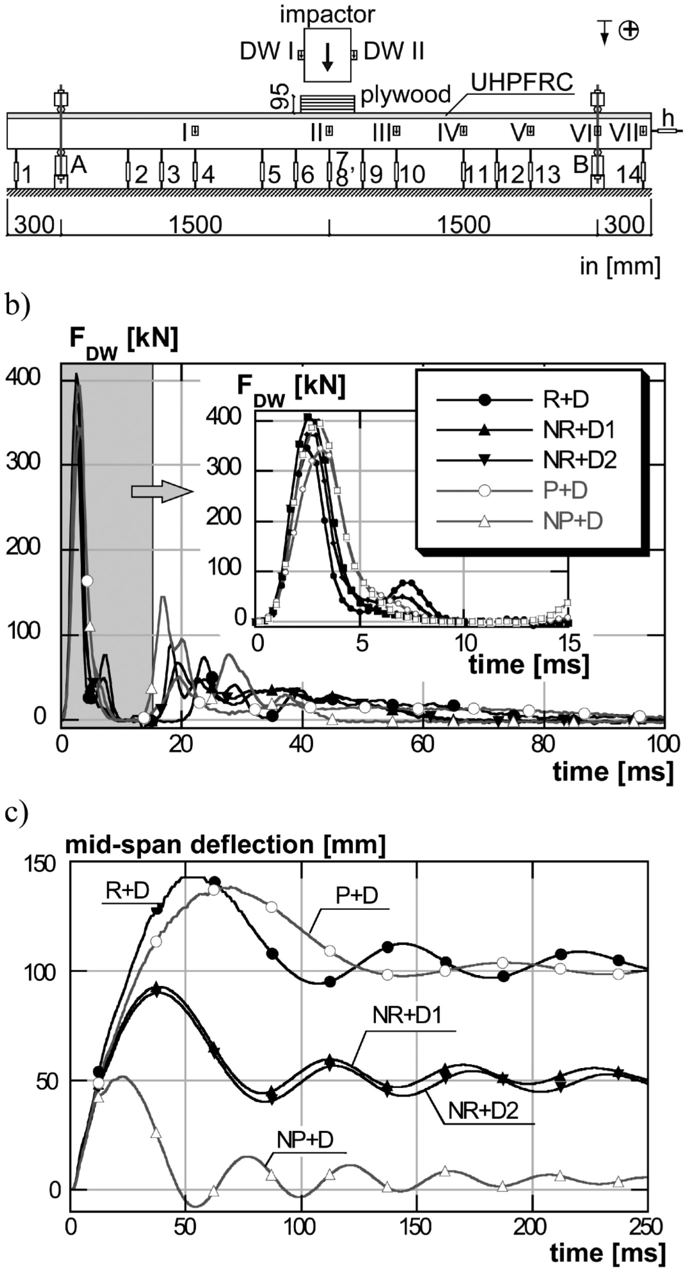


Figure 2. a) Test setup, b) drop weight force $F_{DW}$ vs. time: overview and detail, b) inertia forces.

The slab strips were impacted by a stiff 211 kg weight consisting of a steel case with concrete filling. The drop height was 3.26 m. The weight dropped without noticeable friction, leading to a speed of the drop weight at impact of 8 m/s, which is in the range of low velocity impact or rock fall.

A plywood damper was placed on top of the slab strip at the impact location. The damper was used to reproduce the effect of a cushion layer to the impact such as a layer of asphalt on a bridge deck.

The slab strips were tied down over the supports to prevent uplifting of the slab strips at the supports at all times. Rollers minimized horizontal restraint at the support locations.

Accelerometers (DW I, DW II) on the drop weight were used to directly determine the drop weight force ($F_{DW} = a_{DW} \times m_{DW}$). The slab strips were equipped with displacement transducers (1..14, Fig. 2a), load cells at the supports (A, B) and accelerometers (I..VII). The data acquisition rate was 2.4 kHz for all channels. Further details can be found in Habel & Gauvreau (2009).

Figure 2b shows the drop weight force as a function of time for all slab strips. Its shape was characterized by a main force peak, followed by several lower peaks. The drop weight force became 2 kN (i.e. the static force of the drop weight) between 42 and 100 ms for all slab strips. The maximum drop weight force was between 345 and 410 kN at a time of 2.5 to 3.3 ms.

Figure 2c shows the mid-span deflection versus time for all five slab strips. The magnitude of mid-span deflections is proportional to the degree of damage introduced during the drop weight test. The largest mid-span deflections were reached for the reinforced and post-tensioned slab strips that did not include a UHPFRC layer, R+D and P+D. Identical slab strips NR+D1 and NR+D2 had similar behavior, which proved the repeatability of the tests. The lowest mid-span deflection was obtained for NP+D. Maximum mid-span deflection rates derived from potentiometer readings were 4 to 6 m/s for all specimens.

## 2.4 *Static tests*

Three static three-point bending tests were conducted to investigate the structural response of the slab strips with the UHPFRC overlay in compression as shown in Figure 3a. The static tests served as references to appreciate the effect of high strain rates on the structural response of the members. Details on test method and results can be found in Habel & Gauvreau (2009).

Force-deflection curves of the static tests are shown in Figure 3b. Note that the static test R+S was prematurely stopped at a deflection of 80 mm before fracture and does not reflect the ductility of the slab strip. The addition of a UHPFRC overlay in compression increased the carrying capacity of the slab strip (compare R+S to NR+S), which was mainly due to the increased static height of the member. The post-tensioned slab strip NP+S had the highest carrying capacity and lowest deflection at fracture. This was attributed to the effect of post-tensioning and the increased static height when compared to the reinforced concrete slab strips.

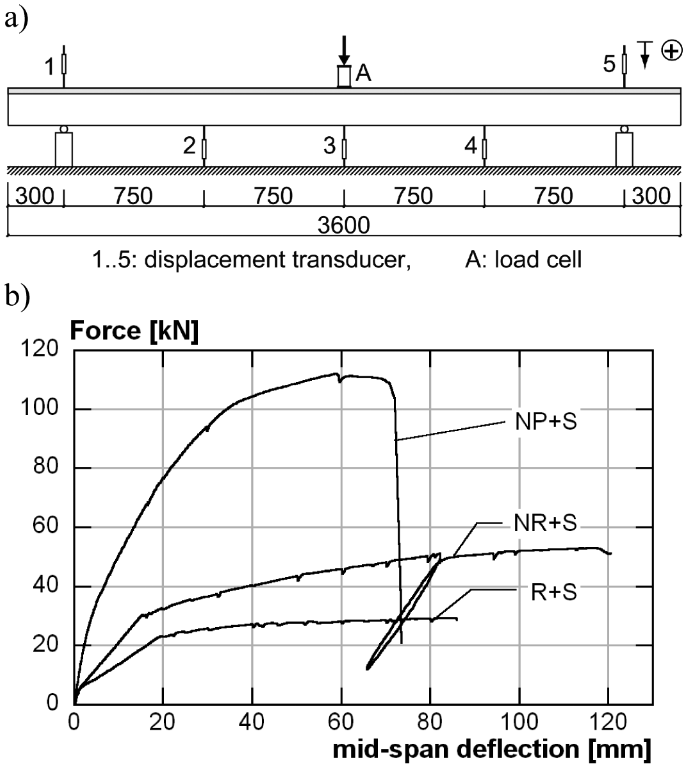


Figure 3. a) Static test setup (UHPFRC in flexural compression shown), b) static force-mid-span deflection curves.

## 3 DYNAMIC EQUILIBRIUM

## 3.1 *Formulation*

The multitude of measurements obtained in the tests – drop weight force deduced from impactor accelerometer measurements, support reactions, specimen displacements and acceleration (see (Habel & Gauvreau 2009)) – allowed establishment and evaluation of the dynamic equilibrium of the slab strips. The dynamic equilibrium, based on Newton's second law of motion, is defined by Equation (1) below and shown graphically in Figure 4.

$$\int_0^L \overline{m}\ddot{u}(x,t)dx + F_{su}(t) - F_{DW}(t) = 0 \qquad (1)$$

where $\overline{m}$ : mass per unit length, $\ddot{u}(x,t)$: acceleration of the slab strip at position x at time t, $F_{su}(t)$: sum of the support reactions at time t, $F_{DW}(t)$: drop weight force at time t.

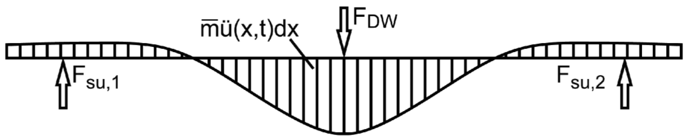


Figure 4. Dynamic equilibrium: schematic view.

The mass per unit length of the slap strips was determined using an assumed specific mass of the reinforced concrete of 2500 kg/m$^3$, a measured specific mass of the UHPFRC of 2660 kg/m$^3$ and the cross sections as shown in Figure 1. The acceleration distribution over the length of the slab strips was determined in two ways: directly from the accelerometer measurements (Fig. 2a), or indirectly from the second derivative with respect to time for deflection measurements from potentiometers. Since all these values were only point measurements, the acceleration values between the measurement locations were linearly interpolated. The sum of the support reactions and the drop weight force were directly obtained by load cell measurements (Fig. 2a). The modeling of the supports assumed infinitely stiff tie-down rods.

## 3.2 *Results*

Calculated inertia forces along slab strip NR+D1 versus time are presented in Figure 5 for a time interval from 1.25 ms and 7.5 ms after the impact of the drop weight. The maximum acceleration forces occurred at 2.5 ms. At this moment, the curve resembled a bell-shape with a maximum force intensity of 30 N/mm in the central region of the beam. Then, the acceleration forces decreased quickly, and the shapes suggest overlapping of several vibration modes with relatively strong damping.

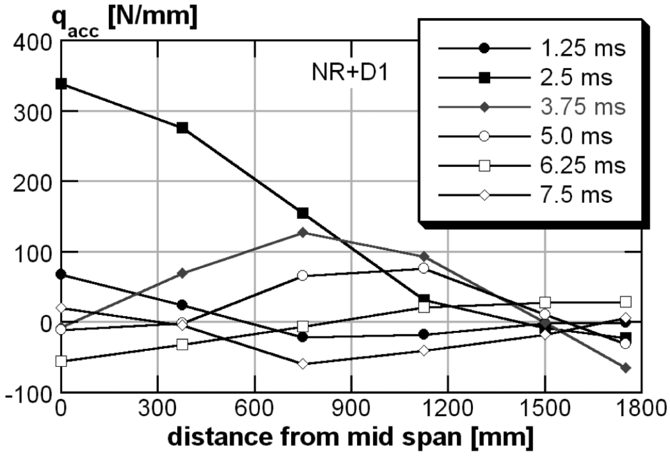


Figure 5. Acceleration forces vs. time for slab strip NR+D1.

Figure 6a provides a comparison between the measured drop weight force (derived from the accelerometers mounted on the drop weight DWI and DWII (see Fig. 2a)) and the drop weight forces calculated with the dynamic equilibrium by considering accelerometer and deflection measurements for slab strip NR+D1. The calculated values were generally in good agreement with the measured drop weight force for both magnitude and time. This was the case for the dynamic equilibrium of all slab strips.

The initial peak of the drop weight force was significantly higher for the calculated values than the measured values (Fig. 6a). Also, the calculated drop weight force curves were less smooth than the measured ones, especially the force derived with the values from the potentiometers. This was attributed to imprecision caused by the interpolations between the measurement points and inaccuracy being created by differentiating the deflection measurement twice with respect to time. Especially in the beginning of the test, the time intervals between each measurement point might have been too large to capture all phenomena in detail.

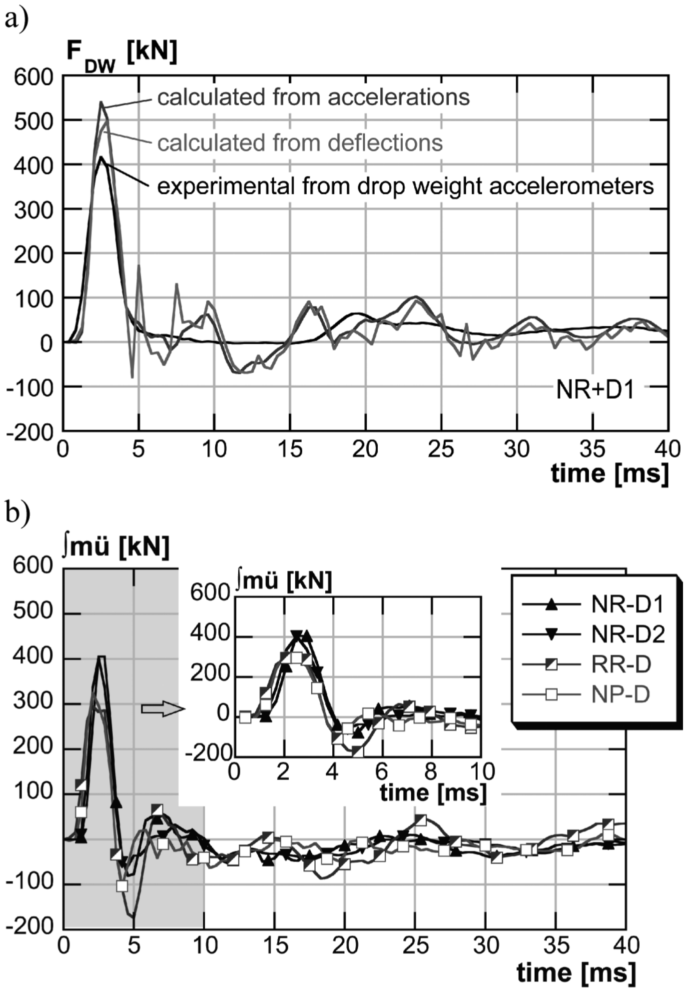


Figure 6. a) Dynamic equilibrium expressed as drop weight force $F_{DW}$ vs. time of NR+D1, b) inertia forces.

The analysis of the dynamic equilibrium demonstrated that the different measurements were consistent. It also showed that the drop weight force could be well derived from acceleration measurements of the drop weight by Newton's second law. However, it was important to obtain the detailed test data to fully monitor the behavior of the slab strips under drop weight loading.

Figure 6b shows the calculated inertia forces for all slab strips tested in the three-point bending system. The inertia forces of slab strip R+D, NR+D1 and P+D were directly calculated from the acceleration measurements. The inertia forces of NR+D2 and NP+D were calculated from the deflection measurements, since the data from the accelerometers was incomplete. The scatter in the measurements was due to inaccuracies in the dynamic equilibrium resulting from the limited number of accelerometers.

The calculations showed significant inertia forces until 7 ms. The maximum forces were highest with values up to 550 kN for the reinforced and post-tensioned slab strips with UHPFRC overlay (NR+D1, NR+D2 and NP+D). Maximum force was around 400 kN for the reinforced and post-tensioned reference slab strips R+D and P+D. The minimum forces were around -100 kN with no significant differences being distinguished between the slab strips.

## 4 MASS-SPRING MODELING

### 4.1 *Formulation*

Dynamic behavior is always characterized by significant inertia effects, as was shown in the previous section. It is well established that the global response of members subjected to impact-type loading can be analyzed with mass-spring models (Biggs 1964, Bischoff et al. 1990, CEB-FIP 1988, Schlüter 1987). A single degree of freedom model, as shown in Figure 7a, was used in this study. The slab strip was modeled as mass $m_B$ onto which the drop weight force $F_{DW}$, obtained from the test results, is applied. The nonlinear spring $R_B$ represented the structural response of the slab strip in form of an equivalent force vs. mid span deflection curve. The mathematical formulation of the model is given in Equation (2):

$$m_B \cdot \frac{d^2 u_B}{dt^2} + R_B(u_B, t) - F_{DW}(t) = 0 \tag{2}$$

with terms according to Figure 7 and t: time.

The model was used to analyze the test results of the reinforced concrete slabs with and without UHPFRC overlay as shown in Figure 7b. The mass $m_B$ corresponded to the equivalent slab strip mass according to Equation (3) (CEB-FIP 1988).

$$m_B = \int_0^L \overline{m} \cdot \Phi^2 \cdot dx \tag{3}$$

where $m_B$: concentrated slab strip mass, $\overline{m}$ : mass per unit length of the specimen, $\Phi$: shape function, L: span length.

The shape function was based on the deflected shape of the specimen. For the current study, the shape function representing the slab strips under quasi-static conditions were utilized. Two cases were considered: linear-elastic beam behavior and the formation of a plastic hinge under the drop weight force at mid span.

The equivalent mass $m_B$ was determined to be 0.42 times the slab strip mass considering linear elastic conditions and 0.32 times the slab strip mass considering a plastic hinge at mid span.

The drop weight force $F_{DW}$ was directly obtained from the results of the drop weight tests described in Habel & Gauvreau (2009). The nonlinear spring $R_B$ corresponded to the equivalent quasi-static force-deflection curve of the slab strip and was obtained through the model. The nonlinear spring $R_B$ was obtained from the static curves, where the force values were adjusted by a scalar factor, while the deformation values were not changed.

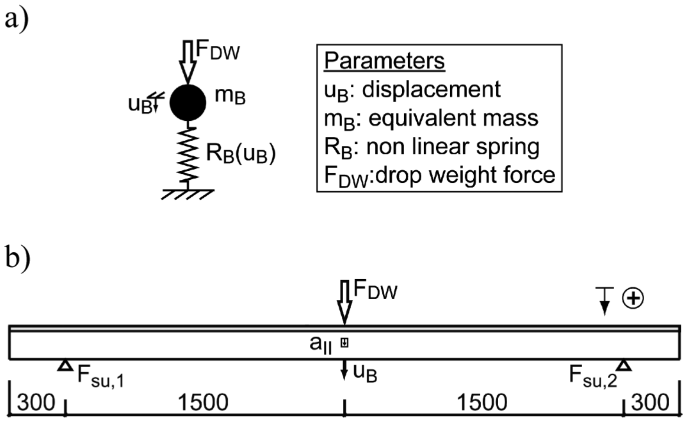


Figure 7. Mass-spring model: a) model definition, and b) application to the slab strips.

It should be noted that the model in its presented form was only capable of simulating the first deflection rise, since it did not consider damping effects. Since the test results show that the first deflection rise was determinant with regard to deflections and cracking of the slab strip, the model was capable of capturing the decisive part of the tests. Damping effects were not incorporated into the model because they would have made the model more complex, whereas it was aimed to validate a simple tool for future design of members under impact-type loading. All slab strips were modeled with the exception of P+D because no static test results existed for this slab strip configuration.

### 4.2 *Drop weight test results*

The drop weight force input based on the experimental results (Habel & Gauvreau 2009) of the concrete slab strips tested in the three-point bending system is shown in Figure 8. The drop weight force was approximated by a multi-linear curve fit. The equivalent mass was 0.32 times the slab strip mass for R+D, 0.36 times the slab strip mass for NR+D1 and NR+D2 and 0.40 times for NP+D. The factors were estimated according to the fracture modes of the slab strips described in (Habel & Gauvreau 2009). R+D had the most concentrated deformation at mid span and was closest to the value assuming a plastic hinge (0.32 x slab strip mass), NR+D1 and NR+D2 showed some indication of deformation localization at mid span, while NP-D was very close to the elastic deflection shape during the modeled first impact and was thus closest to the linear-elastic deflection shape (0.42 x slab strip mass).

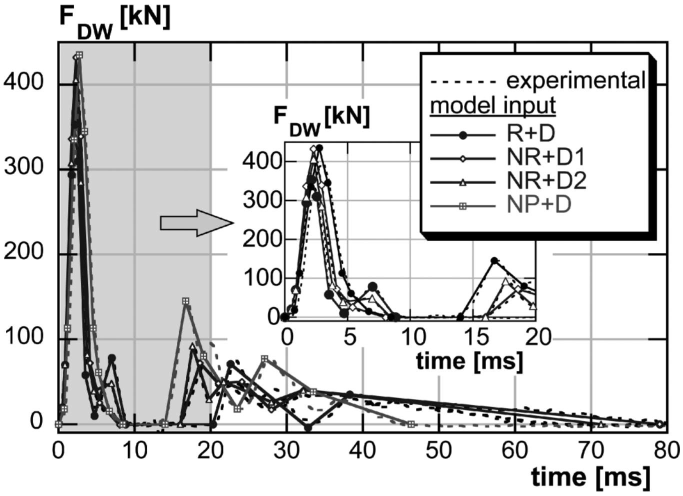


Figure 8. Input data of the mass-spring model for the three-point bending system.

Modeling results are shown in Figure 9. The slab strip deflections under the drop weight were represented well with the model during the first deflection rise, which was the period of validity of the model (Fig. 9a). The obtained quasi-static force-deflection curves, corresponding to the non linear spring $R_B$, are given in Figure 9b. The maximum deflection $u_B$ in Figure 9b is equal to the maximum deflection in Figure 9a. The beginning of the deflection decrease in Figure 9a corresponds to the unloading branch of Figure 9b.

The slope of the unloading branch is steepest for NP+D, and lowest for R+D. This reflects the residual stiffness of the slab strips and is an indication of damage induced into the specimen during the drop weight impact: the steeper the unloading branch, the higher the stiffness after the impact and the lower the damage in the slab strip after the test.

Measured and calculated accelerations of NR+D1 are shown in Figure 9c. The mid-span acceleration $a_B$ obtained by the model was determined from Equation 4.

$$a_B = \frac{d^2 u_B}{dt^2} \tag{4}$$

The modeled acceleration followed well the overall shape of the experimentally obtained acceleration $a_{II}$ (Fig. 9c). The model underestimated the acceleration magnitude measured on the slab strip under the drop weight $a_{II}$ during the first peak at 3 ms. This was attributed to the significant inertia effects, leading to localized deformations and thus higher accelerations under the drop weight. These localized effects could not be captured with the presented model. Beyond 7 ms, the model reproduced the measured accelerations tightly. Similar results for accelerations and support reactions were obtained for all modeled slab strips.

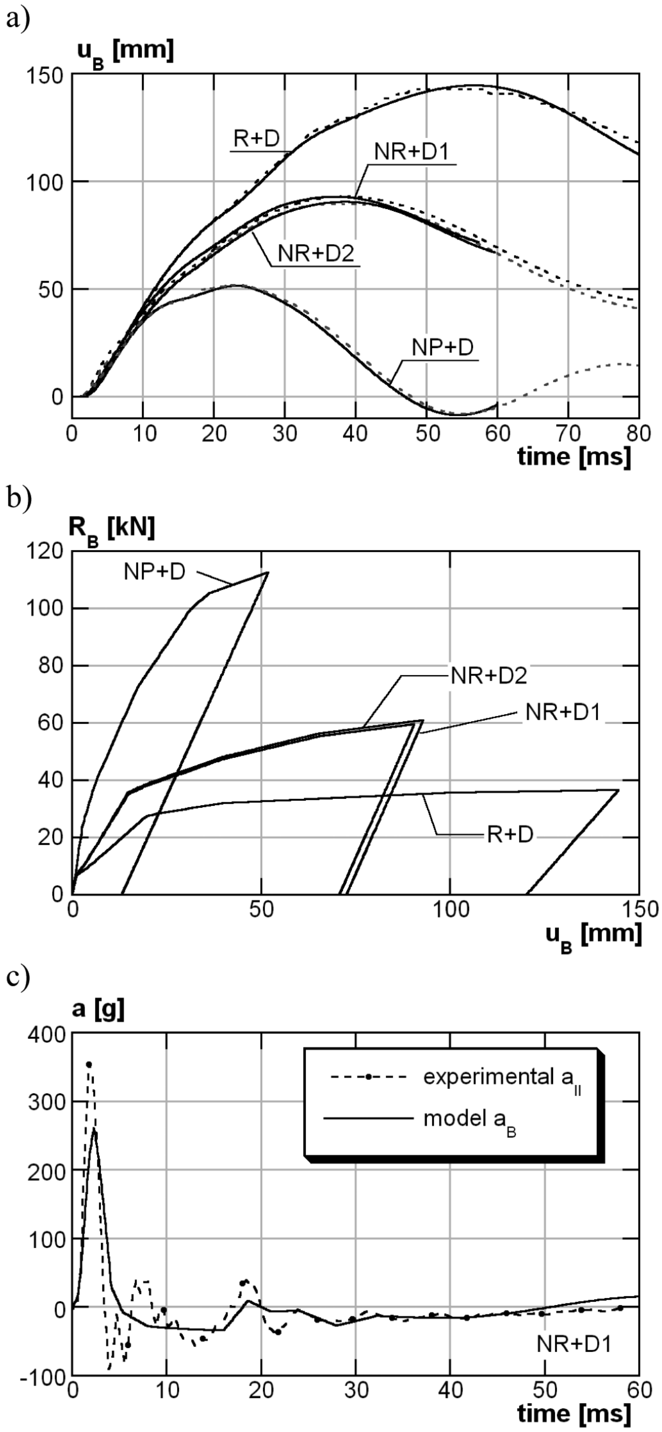


Figure 9. Comparison of modeling and experimental results, a) deflection vs. time, b) nonlinear spring $R_B$ vs. deflection, c), acceleration at mid-span vs. time.

### 4.3 *Comparison of drop weight to static test results*

Figure 10 shows the results of the reference static reinforced concrete slab strips and the drop weight test slab strips with the UHPFRC overlay in flexural compression. Recall that 'S' stands for static and 'D' for equivalent static curves derived from the drop weight tests. It can be seen that the modeled curves of the equivalent static response had higher peak force values than the corresponding quasi-static experimental curves, which is typical for dynamically loaded structural members (e.g. CEB-FIP (1988)). The equivalent peak static force during the drop weight tests was increased by 5% for NP+D. It was 18%, 19%, and 17% for R+D, NR+D1 and NR+D2 respectively, when compared to the force obtained during the corresponding static tests. Recall that the static test R+S was prematurely stopped at a deflection of 80 mm before fracture and does not reflect the ductility of the slab strip.

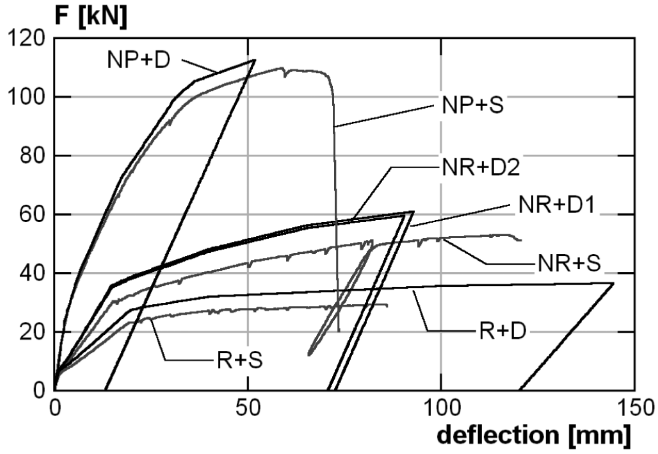


Figure 10. Comparison of modeled and experimental force-deflection curve.

For these slab strips, the UHPFRC overlay was mainly subjected to flexural compression forces. No difference in the amplification factor was observed between the slab strips with and without a UHPFRC overlay. This suggests that UHPFRC in flexural compression had similar changes in mechanical properties under high strain rates as conventional concrete and that the tensile zone of the structural member governs the strength amplification factor. The relatively low amplification factor of the prestressed slab strip NP+D was attributed to the low amount of cracking and high recovery of the slab strip after the first drop as described in Habel & Gauvreau (2009).

## 5 CONCLUSIONS

The analysis of the test results by establishing the dynamic equilibrium and by implementation of a mass-spring model led to the following conclusions:

1. The consistency of the test results was proven by establishing the dynamic equilibrium of the slab strips. It was shown that acceleration, load and deflection measurements were redundant and all valid. Inertia forces up to 550 kN were observed.
2. Analysis with the mass-spring model showed that compared to the static test results, the peak force in the equivalent static force-deflection curve of the drop weight tests when the UHPFRC overlay was mainly in compression was increased by 18% with a reinforced concrete substrate and 5% with a prestressed substrate.
3. In this study, it was demonstrated that simple mass-spring models as presented e.g. in (CEB-FIP 1988) are valid to simulate the global response of slab strips with UHPFRC overlay in flexural compression. The model proved to be valid to simulate the first and main deflection rise due to the impact. However, it was not conceived to reproduce local inertia effects and damping in order to maintain its simplicity.
4. This paper shows that structural members subjected to impact hazards can be designed with mass-spring models to consider both dynamic amplification and rate-dependent material response.

## REFERENCES


Alaee, F.J. & Karihaloo, B. 2003. Retrofitting of Reinforced Concrete Beams with CARDIFRC. *ASCE Journal of Composites for Construction* 7(3): 174-186.

Biggs, J.M. 1964. *Introduction to structural dynamics*, McGraw-Hill, New York, 1964.

Bischoff, P.H., Perry, S.H. & Eibl J. 1990. Contact Force Calculations with a Simple Spring-Mass Model for Hard Impact: A Case Study using Polystyrene Aggregate Concrete. *International Journal of Impact Engineering* 9(3): 317-325.

CEB-FIP. 1988. *Concrete Structures under Impact and Impulsive Loading. Synthesis Report.* Bulletin d'information 187, Lausanne, Switzerland.

Habel, K., Denarié, E. & Brühwiler, E. 2006. Time Dependent Behavior of Elements Combining Ultra-High Performance Fiber Reinforced Concretes (UHPFRC) and Reinforced Concrete, *Materials and Structures* 39(6): 555-567.

Habel, K., Denarié, E. & Brühwiler, E. 2007. Experimental investigation of composite "UHPFRC-concrete" members. *ACI Structural Journal* 104(1): 93-101.

Habel, K., Charron, J-Ph., Braike, S., Hooton, R.D., Gauvreau, P. & Massicotte, B. 2008. Ultra-high performance fibre reinforced concrete (UHPFRC) mix design in Central Canada. *Canadian Journal of Civil Engineering* 35(3): 212-224.

Habel, K. & Gauvreau, P. 2006. Impact behavior of concrete bridge deck slabs with composite ultra-high performance fiber reinforced concrete (UHPFRC) overlay, In *7th International Conference on Short & Medium Span Bridges, Montreal, Canada, August 23-25, 2006* (CD-ROM).

Habel, K. & Gauvreau, P. 2009. Behavior of reinforced and post-tensioned concrete members with a UHPFRC overlay under impact loading. *ASCE Structural Journal* 135(3): 292-300.

Lim, Y.M. & Li, V.C. 1997. Durable repair of aged infrastructures using trapping mechanism of engineered cementitious composites, *Journal of Cement and Concrete Composites* 19(4): 373-385.

Kunieda, M., Kamada, T., Rokugo, K., & Bolander, J.E. 2004. Localized fracture of repair material in patch repair systems, In Victor Li et al. (eds). *Proc. FRAMCOS-5, Vail, Colorado, USA, April-2004:* 765-772.

Maalej, M., Quek, S.T. & Zhang, J. 2005. Behavior of Hybrid - Fiber Engineered Cementitious Composites Subjected to Dynamic Tensile Loading and Projectile Impact. *ASCE Journal of Materials in Civil Engineering* 17(2): 143-152.

Parant, E. & Rossi, P. 2007. Strain Rate Effect on Bending Behavior of New Ultra-high-Performance Cement-Based Composite, *ACI Materials Journal*, 104(5): 458-463.

Schlüter, F.H. 1987. *Dicke Stahlbetonplatten unter stoßartiger Belastung – Flugzeugabsturz. (Reinforced concrete slabs under impact-type loading – airplane crash).* Heft 2, Schriftenreihe des Instituts für Massivbau und Baustofftechnologie, University of Karlsruhe, Germany, 1987.